Sign on

SAO/NASA Astrophysics Data System (ADS)

Bibcode: 1999A&A...346..995S Thumbnails Previous page Next page

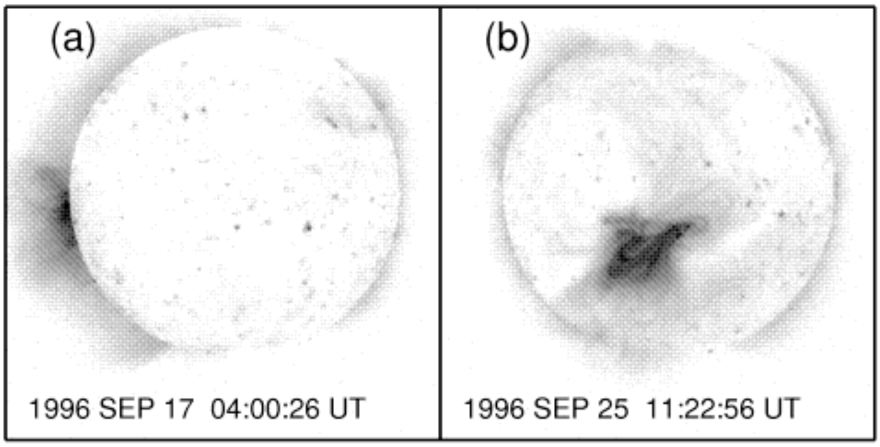

Fig. 1a and b. Images taken with the AlMg filter of SXT **a** when the active region is largely occulted by the east solar limb, and **b** when the region is near disk center. Both images are 5.34 s exposures with SXT's AlMg filter and have $4.91''$ pixel resolution.

disk passage. In subsequent solar rotations, this same activity complex was on the Earthward side of the Sun over the approximate periods July 26—August 9 (when it was re-designated as NOAA 7891), August 22—September 4 (NOAA 7986), September 19—October 2 (too weak for a NOAA designation), and October 17–30 (too weak for a NOAA designation). This is the same region studied by Sterling et al. (1997) as it made its first passage beyond the west solar limb. Hudson et al. (1998) and Harvey & Hudson (1998) discuss other aspects of this same active region.

2. Observations and data analysis

Our observations cover the period 1996 September 10—October 5, which includes the fourth passage of the active region on the disk, including its appearance around the east limb early in that period, and its disappearance around the west limb late in the period. Fig. 1 shows two images from SXT during the period, with west to the right and south downward. Fig. 1a shows the region about two days' rotation behind the east limb and Fig. 1b shows it close to disk-center passage. Both images are 5.34 s exposures with SXT's AlMg filter and have $4.91''$ pixel resolution. Fig. 1b shows that the region is very extended, where the 50%-intensity level covers approximately $600'' \times 450''$. At times during our observation period there also seem to be connections between the brightest parts of the region and surrounding regions, in particular those further to the south.

Yohkoh's BCS (see Culhane et al. 1991 and Lang et al. 1992 for overviews) consists of four channels, covering the resonance lines and principal satellite lines of H-like iron, (Fe XXVI, nominally covering the wavelength range 1.7636–1.8044 Å); He-like iron (Fe XXV, 1.8298–1.8942 Å), He-like calcium (Ca XIX, 3.1631–3.1912 Å), and He-like sulfur (S XV, 5.0160–5.1143 Å). Only the S XV channel covers a low enough energy range to ob-

there is no need for high time cadence. Accordingly, spectra for the data here are for time intervals ranging from 3120 s to 29 448 s in order to obtain statistically-significant spectra.

As in our previous low-flux spectral studies (e.g., Sterling et al. 1997), we addressed the issue of the background in S XV by obtaining spectra at times when there were no active regions on the Sun. We used data accumulated for some 27 000 s on 1996 September 13 for the background, when the active region was on the far side of the Sun prior to the disk passage of this study. The resulting background spectrum is similar to that found by Sterling et al. (1997) in its magnitude, its variation with time, and its wavelength distribution. For example, a background spectrum integrated for about the same length of time from 1996 October 7, which was a time when the region was behind the Sun after the disk passage of this study, has a magnitude within 15% of that of the September 13 background spectrum over the full wavelength range of the S XV channel. Fig. 2a shows the September 13 background spectrum (multiplied by a "background multiplication factor," discussed below, of 0.7), as the lower of the two features in the figure. In the same panel, the upper feature is a spectrum integrated for 21 384 s from a time period when the active region is on the disk. Prominent spectral lines are visible in the upper spectrum, and these lines are strikingly absent in the background spectrum. Since the two spectra were accumulated for a comparable amount of time, this clearly indicates that virtually all the emission-line features in the upper spectrum originate from the weak soft X-ray flux of the active region itself.

There is a wavelength dependence of the background spectrum, which shows a broad intensity peak at wavelengths just short of 5.10 Å. This structured background causes spectra from weak sources to be deformed, and removing some factor times the average background spectrum often improves the shape of the observed spectrum compared to theoretical spectra, as dis-